Inorg. Chem. **2002**, *41*, 1140–1150

Carboxylate and Alkyl Carbonate Coordination at the Hydrophobic Binding Site of Redox-Active Dicobalt Amine Thiophenolate Complexes

Berthold Kersting* and Gunther Steinfeld

Institut für Anorganische und Analytische Chemie, Universität Freiburg, Albertstrasse 21, D-79104 Freiburg, Germany

Received September 25, 2001

A series of new dicobalt complexes of the permethylated macrocyclic hexaamine dithiophenolate ligand H_2L^{Me} have been prepared and investigated in the context of ligand binding and oxidation state changes. The octadentate ligand is an effective dinucleating ligand that supports the formation of bioctahedral complexes with a central $N_3Co(\mu\text{-}SR)_2(\mu\text{-}X)CoN_3$ core structure, leaving a free bridging position X for the coordination of the substrates. The acetato- and cinnamato-bridged complexes $[(L^{Me})Co^{II}_2(\mu\text{-}O_2CMe)]^+$ (**2**) and $[(L^{Me})Co^{II}_2(\mu\text{-}O_2CCH{=}CHPh)]^+$ (**5**) were prepared by reaction of the μ-Cl complex $[(L^{Me})Co^{II}_2(\mu\text{-}Cl)]^+$ (**1**) with the corresponding sodium carboxylates in methanol. The electrochemical properties of these and of the methyl carbonate complex $[(L^{Me})Co^{II}_2(\mu\text{-}O_2COMe)]^+$ (**8**) were also investigated. All complexes undergo two stepwise oxidations at ca. $E^1_{1/2} = +0.22$ and at $E^2_{1/2} =$ ca. +0.60 V vs SCE, affording the mixed-valent complexes $[(L^{Me})Co^{II}Co^{III}(\mu\text{-}O_2CR)]^{2+}$ (**3**, **6**, **9**) and the fully oxidized $Co^{III}Co^{III}$ forms $[(L^{Me})Co^{III}_2(\mu\text{-}O_2CR)]^{3+}$ (**4**, **7**, **10**), respectively. Compounds **3**, **6**, **9** and **4**, **7**, **10** refer to acetato-, cinnamato-, and methylcarbonato species, respectively. The $Co^{II}Co^{III}$ compounds were prepared by comproportionation of the respective Co^{II}_2 and Co^{III}_2 compounds. The $Co^{III}Co^{III}$ species were prepared by bromine oxidation of the $Co^{II}Co^{II}$ forms. The crystal structures of complexes **2**·BPh_4·MeCN, **3**·$(I_3)_2$, **5**·BPh_4·2MeCN, **6**·$(ClO_4)_2$·EtOH, **7**·$(ClO_4)_3$·MeCN·$(H_2O)_3$, and **9**·$(ClO_4)_2$·$(MeOH)_2$·H_2O were determined by single-crystal X-ray crystallography at 210 K. The oxidations occur without gross structural changes of the parent complexes. The $Co^{II}Co^{III}$ complexes are composed of high-spin Co^{II} (d^7) and low-spin Co^{III} (d^6) ions. The $Co^{III}Co^{III}$ complexes are diamagnetic. The oxidation reactions affect the binding mode of the substrates. In the Co^{II}_2 and $Co^{II}Co^{III}$ forms the carboxylates bridge the two Co^{2+} ions in a symmetric μ-1,3 fashion with uniform C–O bond distances, whereas asymmetric bridging modes, with one short C═O and one long C–O distance, are adopted in the fully oxidized species. This is consistent with the observed shifts in vibrational frequencies for ν_{as}(C–O) and ν_s(C–O) across the series.

Introduction

The coordination chemistry of binuclear complexes of first-row transition metal ions has been the subject of extensive investigations in recent years.[1−9] In most cases, the use of binucleating ligands proved to be a powerful strategy for the desired arrangement of the two metal ions (M) and the free coordination sites (X) required for substrate binding.[10−21] A promising strategy to further modulate the

* To whom correspondence should be addressed. E-mail: berthold.kersting@ac.uni-freiburg.de.

(1) Wieghardt, K. *Angew. Chem., Int. Ed. Engl.* **1989**, *28*, 1153−1172.
(2) Que, L.; True, A. E. *Prog. Inorg. Chem.* **1990**, *38*, 97−200.
(3) Feig, A. L.; Lippard, S. J. *Chem. Rev.* **1994**, *94*, 759−805.
(4) Dismukes, G. C. *Chem. Rev.* **1996**, *96*, 2909−2926.
(5) Karlin, K. D.; Kaderli, S.; Zuberbühler, A. D. *Acc. Chem. Res.* **1997**, *30*, 139−147.
(6) Kitajima, N.; Moro-oka, Y. *Chem. Rev.* **1994**, *94*, 737−757.
(7) Solomon, E. I.; Sundaram, U. M.; Machonkin, T. E. *Chem. Rev.* **1996**, *96*, 2563−2605.
(8) Blackman, A. G.; Tolman, W. B. In *Structure & Bonding*; Meunier, B., Ed.; Springer-Verlag: Berlin, 2000; Vol. 97, pp 179−211.
(9) Göbel, M. W. *Angew. Chem., Int. Ed. Engl.* **1994**, *33*, 1141−1143.
(10) Breslow, R. *Acc. Chem. Res.* **1995**, *28*, 146−153.
(11) Suh, J. *Acc. Chem. Res.* **1992**, *25*, 273−279.
(12) Fenton, D. E. *Chem. Soc. Rev.* **1999**, *28*, 159−168.
(13) Bosnich, B. *Inorg. Chem.* **1999**, *38*, 2554−62.
(14) Rapta, M.; Kamaras, P.; Brewer, G. A.; Jameson, G. B. *J. Am. Chem. Soc.* **1995**, *117*, 12865−12866.
(15) Volkmer, D.; Hörstmann, A.; Griesar, K.; Haase, W.; Krebs, B. *Inorg. Chem.* **1996**, *35*, 1132−1135.
(16) Uozumi, S.; Furutachi, H.; Ohba, M.; Okawa, H.; Fenton, D. E.; Shindo, K.; Murata, S.; Kitko, D. J. *Inorg. Chem.* **1998**, *37*, 6281−6287.
(17) Meyer, F.; Kaifer, E.; Kircher, P.; Heinze, K.; Pritzkow, H. *Chem. Eur. J.* **1999**, *5*, 1617−1630.
(18) Barrios, A. M.; Lippard, S. J. *J. Am. Chem. Soc.* **1999**, *121*, 11751−11757.

10.1021/ic011004n CCC: $22.00
Published on Web 02/01/2002

Scheme 1. Modulation of the Chemical Reactivity of Binuclear Complexes by a Local Hydrophobic Microenvironment of the Ligand Matrix[a]

[a] The cavity representation of the ligand $(L^{Me})^{2-}$ should not be confused with the one used for cyclodextrins.[26]

chemical reactivity could be the embedding of the binding site in a local hydrophobic environment (Scheme 1).[22] Complexes of substituted hydrotris(pyrazolyl)borates, in which the substituents serve to form a hydrophobic binding pocket, have already been shown to exhibit enhanced reactivity when compared with their unmodified analogues.[23−25] Complexes of cyclodextrins[26] and calixarenes[26−28] have also been employed for this purpose. In contrast, the study of related binuclear complexes is very limited.[29,30]

We have recently been exploring the coordination chemistry of the macrocyclic amine thiophenolate ligand $(L^{H})^{2-}$ and its permethylated derivative $(L^{Me})^{2-}$. From a structural point of view, the two macrocycles behave in a similar fashion. Both promote the formation of bioctahedral complexes of types A and B, leaving an open position (X) in the bridging region between the two metal ions (Scheme 2).[31] The chemical reactivity of the corresponding complexes, on the other hand, is quite different. Thus, while $[(L^{Me})Ni^{II}_2(\mu\text{-}Cl)]^+$ readily undergoes substitution reactions, complex $[(L^{H})\text{-}Ni^{II}_2(\mu\text{-}Cl)]^+$ of the unmethylated ligand was found to be unreactive.[31] Likewise, the remarkable ability to activate and transform small molecules such as carbon dioxide is restricted to complexes of the permethylated macrocycle.[32] The difference in chemical reactivity has been explained by considering the different environments about the binding sites. So far, our studies have been confined to complexes containing divalent metal ions such as Co^{II}, Ni^{II}, and Zn^{II}. To further develop the coordination chemistry of $(L^{Me})^{2-}$, we decided to prepare and characterize new cobalt(III) complexes.

Scheme 2. Structure of the Ligand H_2L^{Me} and Schematic Representation of the Structures of the Corresponding Metal Complexes $[(L^{Me})M_2(X)]^+$ [a]

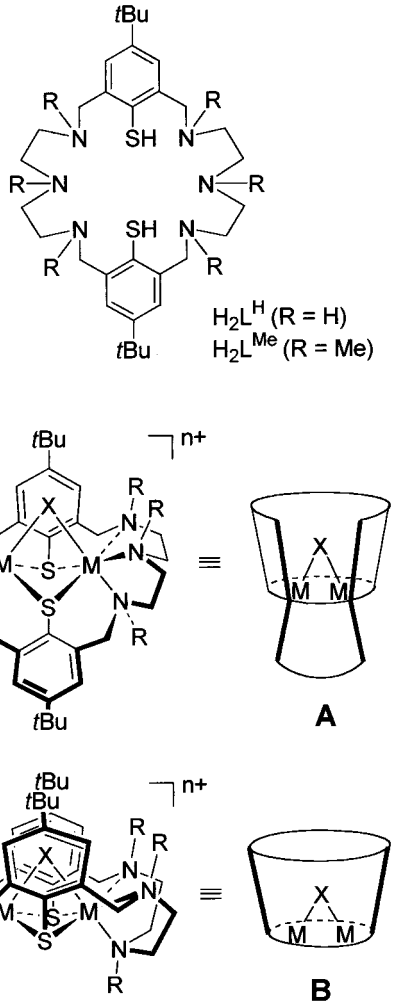

[a] X represents the binding site of the complexes.

A vast number of stable mono- and binuclear Co^{III} amine thiolate complexes have been reported in the literature.[33−40] Our initial characterization of the chloro-bridged dicobalt(II) complex **1**, however, has revealed that the Co^{III} oxidation state is enormously destabilized over the Co^{II} oxidation state in the present complexes. In fact, the Co^{III}_2 form of complex **1** is thermally unstable, even on the time scale of a cyclic voltammetry experiment. As will be seen, the stability of the oxidized species can be greatly increased when the bridging chloro function is replaced by carboxylate coligands. It has also been possible to access Co^{III} complexes of

(19) Barrios, A. M.; Lippard, S. J. *Inorg. Chem.* **2001**, *40*, 1250−1255.
(20) Karlin, K. D.; Zuberbühler, A. D. In *Bioinorganic Catalysis*, 2nd ed. revised and expanded; Reedijk, J., Bouwman, E., Eds.; Marcel Dekker: New York, 1999; pp 469−534.
(21) Incarvito, C.; Rheingold, A. L.; Qin, C. J.; Gavrilova, A. L.; Bosnich, B. *Inorg. Chem.* **2001**, *40*, 1386−1390.
(22) Hecht, S.; Fréchet, J. M. J. *Angew. Chem., Int. Ed.* **2001**, *40*, 74−91.
(23) Trofimenko, S. *Chem. Rev.* **1993**, *93*, 943−980.
(24) Kitajima, N.; Tolman, W. B. *Prog. Inorg. Chem.* **1995**, *43*, 419−531.
(25) Ruf, M.; Vahrenkamp, H. *Inorg. Chem.* **1996**, *35*, 6571−6578.
(26) Reetz, M. T.; Waldvogel, S. R. *Angew. Chem., Int. Ed. Engl.* **1997**, *36*, 865−867.
(27) Wieser-Jeunesse, C.; Matt, D.; De Cian, A. *Angew. Chem., Int. Ed.* **1998**, *37*, 2861−2864.
(28) Blanchard, S.; Le Clainche, L.; Rager, M.-N.; Chansou, B.; Tuchagues, J.-P.; Duprat, A. F.; Le Mest, Y.; Reinaud, O. *Angew. Chem., Int. Ed.* **1998**, *37*, 2732−2735.
(29) Enomoto, M.; Aida, T. *J. Am. Chem. Soc.* **1999**, *121*, 874−875.
(30) Klein Gebbink, R. J. M.; Bosman, A. W.; Feiters, M. C.; Meijer, E. W.; Nolte, R. J. M. *Chem. Eur. J.* **1999**, *5*, 65−69.
(31) Kersting, B.; Steinfeld, G. *Chem. Commun.* **2001**, 1376−1377.
(32) Kersting, B. *Angew. Chem.* **2001**, *113*, 4109−4112; *Angew. Chem., Int. Ed.* **2001**, *40*, 3987−3990.
(33) Jicha, D. C.; Busch, D. H. *Inorg. Chem.* **1962**, *1*, 872−883.
(34) DeSimone, R. E.; Ontko, T.; Wardman, L.; Blinn, E. L. *Inorg. Chem.* **1975**, *14*, 1313−1316.
(35) Beissel, T.; Glaser, T.; Kesting, F.; Wieghardt, K.; Nuber, B. *Inorg. Chem.* **1996**, *35*, 3936−3947.
(36) Kersting, B.; Siedle, G. *Z. Naturforsch., B* **2000**, *55b*, 1179−1187.
(37) Konno, T.; Aizawa, S.; Okamoto, K.; Hidaka, J. *Chem. Lett.* **1985**, 1017−1020.
(38) Okamoto, K.; Aizawa, S.; Konno, T.; Einaga, H.; Hidaka, J. *Bull. Chem. Soc. Jpn.* **1986**, *59*, 3859−3864.
(39) Heeg, M. J.; Blinn, E. L.; Deutsch, E. *Inorg. Chem.* **1985**, *24*, 1118−1120.
(40) Kersting, B.; Siebert, D.; Volkmer, D.; Kolm, M. J.; Janiak, C. *Inorg. Chem.* **1999**, *38*, 3871−3882.

Chart 1. Designation of Cobalt Complexes

$[(L^{Me})Co^{II}{}_2(\mu\text{-}Cl)]^{1+}$	**1**[32]
$[(L^{Me})Co^{II}{}_2(\mu\text{-}O_2CMe)]^{1+}$	**2**
$[(L^{Me})Co^{II}Co^{III}(\mu\text{-}O_2CMe)]^{2+}$	**3**
$[(L^{Me})Co^{III}{}_2(\mu\text{-}O_2CMe)]^{3+}$	**4**
$[(L^{Me})Co^{II}{}_2(\mu\text{-}O_2CCH{=}CHPh)]^{1+,}$	**5**
$[(L^{Me})Co^{II}Co^{III}(\mu\text{-}O_2CCH{=}CHPh)]^{2+,}$	**6**
$[(L^{Me})Co^{III}{}_2(\mu\text{-}O_2CCH{=}CHPh)]^{3+,}$	**7**
$[(L^{Me})Co^{II}{}_2(\mu\text{-}O_2COMe)]^{1+}$	**8**[32]
$[(L^{Me})Co^{II}Co^{III}(\mu\text{-}O_2COMe)]^{2+}$	**9**
$[(L^{Me})Co^{III}{}_2(\mu\text{-}O_2COMe)]^{3+}$	**10**

potentially hydrolyzable substrates such as monomethyl carbonate. The new complexes and their labels are summarized in Chart 1.

We have obtained single crystals of a series of $Co^{II}Co^{II}$, $Co^{II}Co^{III}$, and $Co^{III}Co^{III}$ complexes suitable for X-ray structure determinations. Using infrared spectroscopy with the carboxylates as spectroscopic probes, it has been possible to study the binding modes of the coligands as a function of the metal oxidation states. We are unaware of any other coordinately unsaturated Co_2 thiolate complex that gives information of structural features over an essentially isostructural three-member series of stable complexes.

Experimental Section

Preparation of Compounds. All manipulations were performed under an atmosphere of argon using standard Schlenk techniques. Solvents were purified using conventional methods and were freshly distilled under nitrogen prior to use. The compounds $[(L^{Me})Co^{II}{}_2(\mu\text{-}Cl)]ClO_4$ (**1**·ClO_4) and $[(L^{Me})Co^{II}{}_2(\mu\text{-}O_2COMe)]ClO_4$ (**8**·ClO_4) were prepared using published procedures.[32] Absorption and NMR spectra were determined in acetonitrile solutions unless otherwise noted.

Safety Note! *Perchlorate salts of transition metal complexes are hazardous and may explode. Only small quantities should be prepared with great care.*[41]

$[(L^{Me})Co^{II}{}_2(\mu\text{-}O_2CMe)](ClO_4)$ (2·ClO_4). A solution of sodium acetate (12.3 mg, 0.150 mmol) in methanol (5 mL) was added to a solution of **1**·ClO_4 (92 mg, 0.10 mmol) in methanol (50 mL). The mixture was stirred for 2 h, during which time the color of the solution turned from brown to pale red. A solution of $LiClO_4{\cdot}3H_2O$ (800 mg, 5.00 mmol) in methanol (2 mL) was added. The resulting pale red microcrystalline solid was isolated by filtration, washed with methanol, and dried in air. Yield: 76 mg (80%). mp 327 °C (decomp). Anal. Calcd for $C_{40}H_{67}ClCo_2N_6O_6S_2$: C, 50.81; H, 7.14; N, 8.89; S 6.78. Found: C, 49.72; H, 7.36; N, 8.62; S, 6.20. ^{1}H NMR (CD_3CN): δ = 200.5 (s br, 4H, CH_2), 178.5 (s br, 3H, CO_2CH_3), 147.4 (s br, 4H, CH_2), 132.5 (s, 6H, NCH_3), 77.8 (s br, 4H, CH_2), 76.9 (s, 4H, CH_2), 36.1 (s, 12H, NCH_3), 22.3 (s, 4H, ArH), 8.4 (s, 18H, CH_3), −53.0 (s br, 4H, CH_2), −66.0 (s br, 4H, CH_2). UV/vis (CH_3CN): λ_{max} (ϵ) = 440 nm (467), 523 (170), 542 (sh, 121), 565 (sh, 64), 608 (sh, 21), 1262 (33). IR (KBr, cm^{-1}): $\bar{\nu}$ = 1587 [ν_{as}(C−O)], 1434 [ν_s(C−O)]. The tetraphenylborate salt, $[(L^{Me})Co^{II}{}_2(\mu\text{-}Ac)]BPh_4$ (**2**·BPh_4), was prepared by adding $NaBPh_4$ (342 mg, 1.00 mmol) instead of $LiClO_4$ to the above reaction mixture. IR (KBr, cm^{-1}): $\bar{\nu}$ = 1585 [ν_{as}(C−O)], 1431 [ν_s(C−O)], 732, 703 (BPh_4^-).

$[(L^{Me})Co^{II}Co^{III}(\mu\text{-}O_2CMe)](I_3)_2$ (3·$(I_3)_2$). A solution of I_2 (127 mg, 0.05 mmol) in acetonitrile (25 mL) was added dropwise to a solution of **2**·ClO_4 (95 mg, 0.10 mmol) in acetonitrile (25 mL). The mixture was left to stand in air for 5 days, during which time a few brown-red crystals of **3**·$(I_3)_2$ formed on the bottom of the flask. These crystals were used for an X-ray crystal structure analysis. The compound was not analyzed further because of the low yield.

$[(L^{Me})Co^{II}Co^{III}(\mu\text{-}O_2CMe)](ClO_4)_2$ (3·$(ClO_4)_2$). A solution of **2**·ClO_4 (95 mg, 0.10 mmol) in acetonitrile (25 mL) was added to a solution of **4**·$(ClO_4)_3$ (114 mg, 0.100 mmol) in acetonitrile (25 mL). The reaction mixture was concentrated under vacuum to about 5 mL. An equal amount of ethanol was then added and the brown solution was left to stand in air for 12 h, during which time brown-red crystals of **3**·$(ClO_4)_2$ precipitated. The crystals were isolated by filtration, washed with a little ethanol, and dried in air. Yield: 125 mg (60%). mp >300 °C (decomp). Anal. Calcd for $C_{40}H_{67}Cl_2Co_2N_6O_{10}S_2$: C, 45.98; H, 6.46; N, 8.04; S, 6.14. Found: C, 45.10; H, 6.21; N, 7.73; S, 5.86. UV/vis (CH_3CN): λ_{max} (ϵ) = 456 nm (6434), 710 (1277). IR (KBr, cm^{-1}): $\bar{\nu}$ = 1575 [ν_{as}(C−O)], 1424 [ν_s(C−O)].

$[(L^{Me})Co^{III}{}_2(\mu\text{-}O_2CMe)](ClO_4)_3$ (4·$(ClO_4)_3$). A solution of bromine (80 mg, 0.50 mmol) in acetonitrile (5 mL) was slowly added to a solution of **2**·ClO_4 (190 mg, 0.20 mmol) in acetonitrile (25 mL). During addition the temperature was kept at 0 °C. The resulting dark brown solution was stirred for a further 2 min to ensure complete oxidation of **2**·ClO_4. The reaction mixture was then evaporated to dryness and the brown-black residue redissolved in acetonitrile (10 mL). This procedure was repeated twice more to remove the excess bromine. A solution of $LiClO_4{\cdot}3H_2O$ (800 mg, 5.00 mmol) in ethanol (20 mL) was then added to give a black microcrystalline precipitate. The crystals were filtered, washed with a little ethanol, and dried in air. Yield: 172 mg (75%). mp 300 °C (decomp). Anal. Calcd for $C_{40}H_{67}Cl_3Co_2N_6O_{14}S_2{\cdot}(H_2O)_3$: C, 40.09; H, 6.14; N, 7.01; S, 5.35. Found: C, 39.71; H, 6.23; N, 6.88; S, 4.75. UV/vis (CH_3CN): λ_{max} (ϵ) = 465 nm (12037), 640 (2664). IR (KBr, cm^{-1}): $\bar{\nu}$ = 1525 cm^{-1} [ν_{as}(C−O)], 1427 [ν_s(C−O)]. ^{1}H NMR (CD_3CN, resonances in the region 2.0−4.5 ppm are broad and could not be assigned): δ = 7.31 (s, 4H, ArH), 1.22 (s, 18H, *t*-Bu), 1.00 (s, 3H, CH_3COO^-).

$[(L^{Me})Co^{II}{}_2(\mu\text{-}O_2CCH{=}CHPh)]ClO_4$ (5·ClO_4). A solution of sodium hydroxide (12 mg, 0.30 mmol) in methanol (1 mL) was added to a solution of cinnamic acid (44 mg, 0.30 mmol) in methanol (10 mL). This solution was then added to a solution of **1**·ClO_4 (160 mg, 0.174 mmol) in methanol (30 mL), and the reaction mixture stirred for 2 h. The resulting pale red precipitate was filtered, washed with 1 mL of cold methanol, and dried in air. Yield: 168 mg (81%). mp 334 °C (decomp). Anal. Calcd for $C_{47}H_{71}ClCo_2N_6O_6S_2$: C, 54.62; H, 6.92; N, 8.13; S, 6.20. Found: C, 53.55; H, 7.07; N, 7.89; S, 5.76. ^{1}H NMR (CD_3CN): δ = 199.0 (s br, 4H, CH_2), 185.7 (s br, 1H, C*H*═CHPh), 145.2 (s br, 4H, CH_2), 134.4 (s, 6H, NCH_3), 106.9 (s, 1H, CH═C*H*Ph), 77.8 (s, 4H, CH_2), 76.8 (s br, 4H, CH_2), 39.81 (s, 2H, CH═CHAr*H*), 37.3 (s, 12H, NCH_3), 23.4 (s, 4H, ArH), 18.76 (s, 2H, CH═CHAr*H*), 18.72 (s, 1H, CH═CHAr*H*), 8.5 (s, 18H, CH_3), −51.0 (s br, 4H, CH_2), −69.0 (s br, 4H, CH_2). UV/vis (CH_3CN): λ_{max} (ϵ) = 445 nm (487), 524 (193), 544 (sh, 138), 567 (sh, 80), 606 (sh, 36), 1259 (43). IR (KBr, cm^{-1}): $\bar{\nu}$ = 1642 [ν(C═C)], 1576 [ν_{as}(C−O)], 1407 [ν_s(C−O)]. The tetraphenylborate salt, [(L^{Me})-

(41) Wolsey, W. C. *J. Chem. Educ.* **1973**, *50*, A335−A337.

Table 1. Crystallographic Data for Compounds Containing Complexes **2**, **3**, **5**, **6**, **7**, and **9**

	2·BPh_4·MeCN	**3**·$(I_3)_2$	**5**·BPh_4·2MeCN	**6**·$(ClO_4)_2$·EtOH	**7**·$(ClO_4)_3$·MeCN·$(H_2O)_3$	**9**·$(ClO_4)_2$·$(MeOH)_2$·H_2O
formula	$C_{66}H_{90}BCo_2N_7O_2S_2$	$C_{40}H_{67}Co_2I_6N_6O_2S_2$	$C_{75}H_{97}BCo_2N_8O_2S_2$	$C_{49}H_{77}Cl_2Co_2N_6O_{11}S_2$	$C_{49}H_{80}Cl_3Co_2N_7O_{17}S_2$	$C_{42}H_{77}Cl_2Co_2N_6O_{14}S_2$
fw	1206.24	1607.38	1335.40	1179.05	1327.53	1142.98
space group	$P\bar{1}$	$P\bar{1}$	$P\bar{1}$	$P\bar{1}$	Pbca	$P2_1/c$
a, Å	13.319(3)	10.668(2)	13.191(3)	15.457(3)	16.003(3)	16.617(3)
b, Å	15.628(3)	13.913(3)	15.164(3)	18.421(4)	23.209(5)	20.232(4)
c, Å	16.997(3)	19.424(4)	19.734(4)	20.665(4)	37.134(7)	15.717(3)
α, deg	108.38(3)	84.48(3)	74.69(3)	96.27(3)		
β, deg	92.24(3)	87.82(3)	83.59(3)	91.86(3)		93.54(3)
γ, deg	107.38(3)	69.94(3)	78.59(3)	105.69(3)		
V	3169(1)	2695.5(9)	3725(1)	5619(2)	13792(5)	5274(2)
Z	2	2	2	4	8	4
ρ_{calcd}, g/cm^3	1.264	1.980	1.191	1.394	1.279	1.440
temp, K	210(2)	210(2)	210(2)	210(2)	210(2)	210(2)
μ(Mo Kα), mm^{-1}	0.638	4.166	0.550	0.821	0.720	0.876
2θ limits, deg	3−57	3−57	3−57	2−57	2−57	2−57
total no. data	28 252	24 448	33 767	51 311	85 015	33 380
no. unique data	14 915	12 603	17 419	26 212	16 862	12 663
obsd. data[a]	7050	8868	11957	7800	2431	3270
no. params	702	523	766	1115	724	548
R[b]	0.0453	0.0343	0.0565	0.0726	0.0913	0.0681
wR2[c]	0.0868	0.0904	0.1930	0.1798	0.2421	0.1701
max, min peaks, e/Å^3	0.529/−0.529	1.850/−1.259	1.249/−0.843	1.088/-0.813	1.092/−0.714	0.989/−0.572

[a] Observation criterion: $I > 2\sigma(I)$. [b] $R1 = \sum||F_o| - |F_c||/\sum|F_o|$. [c] $wR2 = \{\sum[w(F_o^2 - F_c^2)^2]/\sum[w(F_o^2)^2]\}^{1/2}$.

$Co^{II}_2(\mu\text{-}O_2CCH{=}CHPh)]BPh_4$ (**5**·BPh_4), was prepared by adding $NaBPh_4$ (342 mg, 1.00 mmol) instead of $LiClO_4$ to the above reaction mixture. IR (KBr, cm^{-1}): $\bar{\nu}$ = 1642 [ν(C=C)], 1576 [ν_{as}(C−O)], 1406 [ν_s(C−O)], 732, 703 (BPh_4^-).

[(L^{Me})$Co^{II}Co^{III}$(μ-$O_2CCH{=}CHPh$)](ClO_4)$_2$ (6·(ClO_4)$_2$). This complex was prepared by a method analogous to that described above for **3**·(ClO_4)$_2$. The compounds **5**·ClO_4 (103 mg, 0.100 mmol) and **7**·(ClO_4)$_3$ (123 mg, 0.100 mmol) were used instead of **2**·ClO_4 and **4**·(ClO_4)$_3$, respectively. Yield: 125 mg (55%). mp >300 °C (decomp). Anal. Calcd for $C_{47}H_{71}Cl_2Co_2N_6O_{10}S_2$: C, 49.82; H, 6.32; N, 7.42; S, 5.66. Found: C, 50.14; H, 6.24; N, 7.33; S, 5.28. UV/vis (CH_3CN): λ_{max} (ϵ) = 458 nm (6604), 710 (1330). IR (KBr, cm^{-1}): $\bar{\nu}$ = 1635 [ν(C=C)], 1558 [ν_{as}(C−O)], 1391 [ν_s(C−O)].

[(L^{Me})Co^{III}_2(μ-$O_2CCH{=}CHPh$)](ClO_4)$_3$ (7·(ClO_4)$_3$). This compound was prepared by the same method as described above for **4**·(ClO_4)$_3$. Compound **5**·ClO_4 (207 mg, 0.200 mmol) was used instead of **2**·ClO_4. Yield: 205 mg (83%). mp >300 °C (decomp). Anal. Calcd for $C_{47}H_{71}Cl_3Co_2N_6O_{14}S_2$: C, 45.80; H, 5.81; N, 6.82; S, 5.20. Found: C, 44.31; H, 5.12; N, 7.32; S, 5.11. UV/vis (CH_3CN): λ_{max} (ϵ) = 467 nm (11 598), 637 (2593). IR (KBr, cm^{-1}): $\bar{\nu}$ = 1631 [ν(C=C)], 1508 [ν_{as}(C−O)], 1388 [ν_s(C−O)]. ^{1}H NMR (DMSO-d_6, resonances in the region 4.5−2.0 are broad and could not be assigned): δ = 7.38−7.30 (m, 9H), 6.63 (d, J = 16 Hz, 1H), 5.84 (d, J = 16 Hz, 1H), 4.11 (m), 3.88 (m), 3.52 (m), 3.47 (s br), 3.09 (s br), 3.03 (s br), 2.95 (s br), 2.88 (s br), 2.78 (s br), 2.65 (s br), 1.10 (s, 18H). ^{13}C NMR (DMSO-d_6): δ = 181.6 (RCO_2), 158.0, 153.5, 149.7, 142.9 (CH), 135.5 (CH), 133.2 (CH), 131.9 (CH), 128.9 (CH), 118.9 (CH), 66.2 (CH_2), 64.9 (CH_2), 62.2 (CH), 55.0, 48.5, 34.6, 30.0.

[(L^{Me})$Co^{II}Co^{III}$(μ-O_2COMe)](ClO_4)$_2$ (9·(ClO_4)$_2$). This compound was prepared by the same method described above for **3**·(ClO_4)$_2$. Compounds **8**·ClO_4 (96 mg, 0.100 mmol) and **10**·(ClO_4)$_3$ (116 mg, 0.100 mmol) were used instead of **2**·(ClO_4) and **4**·(ClO_4)$_3$. The product was recrystallized from CH_3CN/MeOH. Yield: 125 mg (54%). mp >300 °C (decomp). Anal. Calcd for $C_{40}H_{67}Cl_2Co_2N_6O_{11}S_2$: C, 45.29; H, 6.37; N, 7.92; S, 6.05. Found: C, 44.78; H, 5.90; N, 7.66; S, 5.81. UV/vis (CH_3CN): λ_{max} (ϵ) = 450 nm (5944), 684 (1287); IR (KBr): $\bar{\nu}$ =1635 cm^{-1} [ν_{asym}(C−O)], 1344 [ν_{sym}(C−O)].

[(L^{Me})Co^{III}_2(μ-O_2COMe)](ClO_4)$_3$ (10·(ClO_4)$_3$). This compound was prepared by the same method as described above for **4**·(ClO_4)$_3$, except that the product was recrystallized from CH_3CN/MeOH. Compound **8**·ClO_4 (192 mg, 0.200 mmol) was used instead of **2**·(ClO_4). Yield: 124 mg (58%). mp >290 °C (decomp). Anal. Calcd for $C_{40}H_{67}Cl_3Co_2N_6O_{15}S_2$: C, 41.40; H, 5.82; N, 7.24; S, 5.53. Found: C, 40.55; H, 5.67; N, 7.13; S, 5.22. UV/vis (CH_3CN): λ_{max} (ϵ) = 466 nm (9000), 643 (2048). IR (KBr): $\bar{\nu}$ = 1556 cm^{-1} [ν_{as}(C−O)], 1353 [ν_s(C−O)]. CV (CH_3CN, 295 K, 0.1 M n-Bu_4NPF_6, 100 mV·s^{-1}; E (V) vs SCE): $E^1_{1/2}$ = +0.26 (ΔE_p = 0.137 V); $E^2_{1/2}$ = +0.66 (0.200).

Collection and Reduction of X-ray Data. Single crystals of **2**·BPh_4·MeCN, **3**·$(I_3)_2$, and **9**·$(ClO_4)_2$·2MeOH·H_2O were taken directly from the reaction mixtures. Crystals of **5**·BPh_4·2MeCN and of **6**·$(ClO_4)_2$·EtOH were grown by slow evaporation of solutions of the complexes in acetonitrile/ethanol (1:2) mixed-solvent systems. Black crystals of **7**·$(ClO_4)_3$·MeCN·$3H_2O$ were grown by slow evaporation of a solution of the complex in acetonitrile. The crystals were mounted on the tips of glass fibers using perfluoropolyether oil. Intensity data were collected at 210(2) K, using a Bruker CCD X-ray diffractometer. Graphite monochromated Mo Kα radiation (λ = 0.710 73 Å) was used. Crystallographic data of the compounds are listed in Table 1. The data were processed with SAINT[42] and corrected for absorption using SADABS[43] (transmission factors 1.00−0.90 (**2**), 1.00−0.79 (**3**), 1.00−0.86 (**5**), 1.00−0.88 (**6**), 1.00−0.59 (**7**), 1.00−0.89 (**9**)). The structures were solved by using the program SHELXS-86.[44] Refinements were carried out with the program SHELXL-93.[45] PLATON was used to search for higher symmetry.[46] ORTEP-3 was used for the artwork of the structures.[47] All non-hydrogen atoms were refined anisotropically, except for those of the disordered *t*-Bu groups, the solvent molecules of

(42) *SAINT+*, V6.02; Bruker AXS; Madison, WI, 1999.
(43) Sheldrick, G. M. *SADABS, Area-Detector Absorption Correction*; University of Göttingen: Göttingen, Germany, 1996.
(44) Sheldrick, G. M. *Acta Crystallogr., Sect. A* **1990**, *A46*, 467−473.
(45) Sheldrick, G. M. *SHELXL-93*, Computer program for crystal structure refinement; University of Göttingen: Göttingen, Germany, 1993.
(46) Spek, A. L. *PLATON—A Multipurpose Crystallographic Tool*; Utrecht University: Utrecht, The Netherlands, 2000.
(47) Farrugia, L. J. *J. Appl. Crystallogr.* **1997**, *30*, 565.

crystallization, and the aryl ring of the cinnamate ion from molecule A in **6**. The O atoms of all ClO_4^- anions in **6** and of the disordered one in **7** were refined isotropically. Hydrogen atoms were assigned to idealized positions and given isotropic thermal parameters 1.2 times (1.5 times for CH_3 groups) the thermal parameter of the atoms to which they were attached. Split atom models were used to account for the disorder of *tert*-butyl groups in complexes **2**, **6**, **7**, and **9**. The site occupancies of the two positions were refined as follows: C(32a)−C(34a)/C(32b−C(34b) 0.56(1)/0.44(1) for **2**, 0.55(3)/0.45(3) for **6**, and 0.55(5)/0.45(5) for **7**; and C(36a)−C(38a)/C(36b)−C(38b) 0.55(1)/0.45(1) for **2** and 0.63(2)/0.37(2) for **9**. In the structure of **7**, one ClO_4^- anion is disordered over two positions. The site occupancies of the two positions were refined as follows: O(11a)−O(14a)/O(11b)−O(14b): 0.66(2)/0.34(2).

Other Physical Measurements. Infrared spectra were recorded over the range 4000−400 cm^{-1} on a Bruker VECTOR 22 FT-IR spectrophotometer using KBr pellets. Melting points were determined in capillaries and are uncorrected. ^1H NMR and ^{13}C NMR spectra were recorded on a Bruker AVANCE DPX-200 spectrometer. Electronic absorption spectra were recorded on a Jasco V-570 UV/vis/near-IR spectrophotometer (range 400−1600 nm). Elemental analyses were performed on a Vario EL analyzer (Elementaranalysensysteme GmbH). Cyclic voltammetry measurements were carried out at 25 °C with an EG&G Princeton Applied Research potentiostat/galvanostat Model 263 A. The cell contained a Pt working electrode, a Pt wire auxiliary electrode, and an Ag wire as reference electrode. Sample concentration was ca. 1.0×10^{-3} M in 0.10 M $[n\text{-}Bu_4N]PF_6$ supporting electrolyte. Cobaltocenium hexafluorophosphate was used as internal standard (under our experimental conditions, the $Co(Cp)_2^+/Co(Cp)_2$ couple is at $E_{1/2} = -1.345$ V vs the $Fe(Cp)_2^+/Fe(Cp)_2$ couple). All potentials were converted to the SCE reference using tabulated values.[48]

Results and Discussion

Synthesis of Carboxylato-bridged Cobalt(II) Complexes. The chloro-bridged complex $[(L^{Me})Co^{II}_2(\mu\text{-}Cl)]^+$ (**1**) was found to be an excellent starting material for the preparation of the carboxylato-bridged dicobalt(II) complexes **2** and **5**. Compound **1** reacted smoothly with 1.5 equiv of sodium acetate or sodium cinnamate in methanol at room temperature (eq 1) to produce a pale red solution. Upon

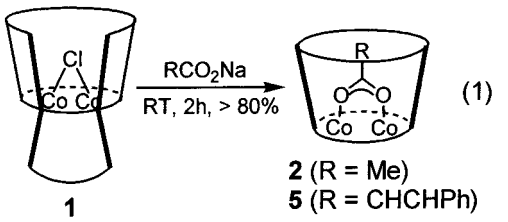

addition of $LiClO_4 \cdot 3H_2O$, the pale red complex $[(L^{Me})Co^{II}_2(\mu\text{-}O_2CMe)]ClO_4$ (**2**·ClO_4) or $[(L^{Me})Co^{II}_2(\mu\text{-}O_2CCH{=}CHPh)]ClO_4$ (**5**·ClO_4), respectively, precipitated with a high yield. Addition of $NaBPh_4$ instead of $LiClO_4$ gave the corresponding tetraphenylborate salts **2**·BPh_4 and **5**·BPh_4. The new compounds exhibit good solubility in acetonitrile, but they are only sparingly soluble in alcohols and virtually insoluble in halogenated hydrocarbons. Unlike the chloro-bridged complex **1**, all are stable in air, even in solution.

The electrochemical properties of the dicobalt(II) complexes described below implied that the oxidized $Co^{II}Co^{III}$ and $Co^{III}Co^{III}$ forms would be amenable to isolation using mild oxidants. Initial attempts to prepare the mixed-valent $Co^{II}Co^{III}$ complex **3** focused on the chemical oxidation of the acetato-bridged derivative **2**·ClO_4 with iodine. The reaction in eq 2 was accompanied by a color change from pale red to red-brown, indicating the formation of the desired $Co^{II}Co^{III}$ species. However, all attempts to isolate a perchlorate salt have failed. In one case, a few crystals of composition $[(L^{Me})Co^{II}Co^{III}(\mu\text{-}O_2CMe)](I_3)_2$ (**3**·$(I_3)_2$)—just enough for a single-crystal X-ray diffraction study—were obtained. The crystal structure determination unambiguously revealed the presence of a mixed-valent $Co^{II}Co^{III}$ complex (see below). Nevertheless, the yield was low and a more convenient synthetic procedure was highly desirable.

The comproportionation reaction between **2**·ClO_4 and the fully oxidized $Co^{III}Co^{III}$ species **4**·$(ClO_4)_3$ (see below) was sought as an alternative route. As shown in eq 3, **2** reacted smoothly with **4** in acetonitrile at 0 °C to give, after evaporation of the solvent and recrystallization from CH_3CN/EtOH, the isolated mixed-valent complex **3**·$(ClO_4)_2$ in 60% yield. Complex **6**·$(ClO_4)_2$ could also be readily prepared in this manner. The complexes were isolated as air-stable, dark brown microcrystalline powders. Our observations indicate that this latter method is a decisively cleaner and more general protocol than the previous one. Similarly to their parent complexes, compounds **3**·$(ClO_4)_2$ and **6**·$(ClO_4)_2$ exhibit excellent solubility in polar-aprotic media such as acetonitrile to give deep brown solutions, while they are practically insoluble in ethanol or methanol. In the absence of reducing agents, acetonitrile solutions of the $Co^{II}Co^{III}$ complexes can be stored for several days at ambient temperature without noticeable decomposition.

The preparation of the fully oxidized $Co^{III}Co^{III}$ complexes was attempted next. The addition of an excess of bromine to solutions of the perchlorate salts of the dicobalt(II) complexes in acetonitrile at 0 °C, followed by addition of an excess of $LiClO_4$ and recrystallization of the resulting solid from $EtOH/CH_3CN$, was found to be the method of choice. In the case of **2**·ClO_4, a black solid of composition $[(L^{Me})Co^{III}_2(\mu\text{-}O_2CMe)](ClO_4)_3$ (**4**·$(ClO_4)_3$) could be isolated with a 72% yield, eq 4. The Br_2 oxidation of **5**·ClO_4 produced

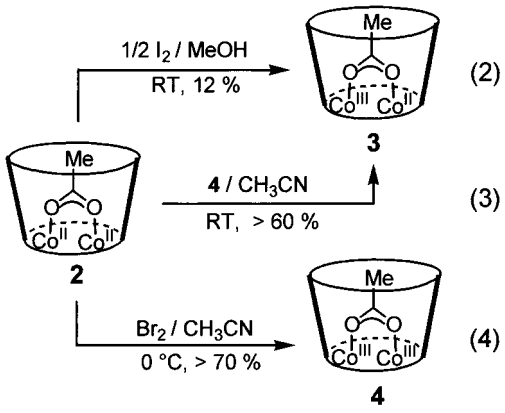

(48) Connelly, N. G.; Geiger, W. E. *Chem. Rev.* **1996**, *96*, 877−910.

Table 2. Electrochemical Data, E (V), for **1**−**12**[a]

no.	compound	$E^1_{1/2}$ (III,II/II,II)[b]	$E^2_{1/2}$ (III,III/III,II)[b]	ΔE[c]	K_c[d]
1[e]	$[(L^{Me})Co^{II}_2(\mu\text{-}Cl)]^+$	0.47 (0.136)	0.97 (irr.)		
2	$[(L^{Me})Co^{II}_2(\mu\text{-}O_2CMe)]^+$	0.21 (0.118)	0.60 (0.147)	0.39	
3	$[(L^{Me})Co^{II}Co^{III}(\mu\text{-}O_2CMe)]^{2+}$	0.22 (0.122)	0.60 (0.147)	0.38	2.7×10^6
4	$[(L^{Me})Co^{III}_2(\mu\text{-}O_2CMe)]^{3+}$	0.22 (0.122)	0.60 (0.150)	0.38	
5	$[(L^{Me})Co^{II}_2(\mu\text{-}O_2CR)]^+$	0.20 (0.120)	0.58 (0.130)	0.38	
6	$[(L^{Me})Co^{II}Co^{III}(\mu\text{-}O_2CR)]^{2+}$	0.20 (0.120)	0.57 (0.130)	0.37	1.8×10^6
7	$[(L^{Me})Co^{III}_2(\mu\text{-}O_2CR)]^{3+}$	0.20 (0.120)	0.60 (0.129)	0.40	
8	$[(L^{Me})Co^{II}_2(\mu\text{-}O_2COMe)]^+$	0.26 (0.125)	0.66 (0.180)	0.40	
9	$[(L^{Me})Co^{II}Co^{III}(\mu\text{-}O_2COMe)]^{2+}$	0.26 (0.121)	0.66 (0.187)	0.40	
10	$[(L^{Me})Co^{III}_2(\mu\text{-}O_2COMe)]^{3+}$	0.26 (0.137)	0.66 (0.200)	0.40	
11[f]	$[(L')_3Co^{III}_2]^{n+}$	−0.85 (0.127)	−0.47 (0.132)	0.38	2.6×10^6
12[f]	$[(L'')Co^{III}_2]^{n+}$	−0.84 (0.136)	−0.40 (0.119)	0.44	2.8×10^6

[a] Data recorded using the perchlorate salts in CH_3CN solution. All potentials are referenced to SCE. For experimental conditions see the Experimental Section. [b] $E^x_{1/2} = (E^{ox}_p + E^{red}_p)/2$ for reversible one-electron-transfer processes; values in parentheses represent peak-to-peak separations ($\Delta E_p = |E^{ox}_p - E^{red}_p|$). [c] $\Delta E^x_{1/2} = |E^1_{1/2} - E^2_{1/2}|$. [d] $K_c = \exp(38.94\Delta E^x_{1/2})$, at 298 K. [e] Reference 32. [f] Reference 40.

$[(L^{Me})Co^{III}_2(\mu\text{-}O_2CCH{=}CHPh)](ClO_4)_3$ (**7**·$(ClO_4)_3$) in a similar good yield (75%). The solubilities of the two fully oxidized complexes were not as good as those of **3**·$(ClO_4)_2$ and **6**·$(ClO_4)_2$.

Synthesis of μ-Alkyl Carbonato Complexes 9 and 10. The bridging methyl carbonate group in complex $[(L^{Me})Co^{II}_2(\mu\text{-}O_2COMe)]^+$ (**8**) is, unlike the carboxylates in **2** and **5**, a potentially hydolyzable substrate. As can be seen in eq 5, treatment of **8** with an excess of bromine, using reactions

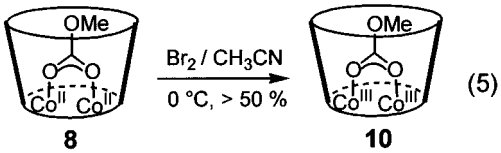

8 **10**

conditions similar to those described above for **4**, produced the $Co^{III}Co^{III}$ complex **10** in good yields. Likewise, oxidation of **8** with **10** yielded the mixed-valent $Co^{II}Co^{III}$ form **9**. These results demonstrate that all three members of this series are also readily available.

It is noted that the oxidations are chemically reversible. Thus, addition of suitable reducing agents such as $NaBH_4$ to either the $Co^{II}Co^{III}$ or the $Co^{III}Co^{III}$ species re-forms the parent $Co^{II}Co^{II}$ complexes. The new compounds gave satisfactory elemental analyses and were characterized by cyclic voltammetry, spectroscopic methods (UV/vis, ^{1}H NMR, and infrared spectroscopy), and, where possible, single-crystal X-ray diffraction analyses.

Electrochemistry. All complexes were characterized by cyclic voltammetry. Cyclic voltammograms have been recorded in CH_3CN solution with $[Bu_4N][PF_6]$ as the supporting electrolyte. All potentials reported are referenced versus SCE. The electrochemical data are summarized in Table 2.

The cyclic voltammogram (CV) of **2**·(ClO_4) displays two reversible redox waves at $E^1_{1/2} = +0.22$ V ($\Delta E_p = 122$ mV) and $E^2_{1/2} = +0.60$ V ($\Delta E_p = 150$ mV) vs SCE (Figure S1, Supporting Information). The CVs of **3**·$(ClO_4)_2$ and **4**·$(ClO_4)_3$ using the same experimental conditions are identical within experimental error. Thus, the reversible oxidation at E^1 is assigned to the one-electron oxidation of the $Co^{II}Co^{II}$ form to the mixed-valent $Co^{II}Co^{III}$ form **3**, and the second redox wave at E^2 is assigned to the oxidation of the mixed-valent $Co^{II}Co^{III}$ form to the fully oxidized $Co^{III}Co^{III}$ form **4**. The CVs of the other two cobalt complexes, **5**·(ClO_4) and **8**·(ClO_4), show, as expected, only very small differences from that of **2**·(ClO_4) (Table 2). Again, the CVs of their oxidized derivatives are identical within experimental error.

Table 3. Selected UV/vis and Infrared Spectroscopic Data for Compounds **1**−**10**[a]

no.	λ_{max}/nm (ϵ/M^{-1} cm^{-1})[b]	ν_{as}, ν_s (CO_2)	Δ[c]
1[d]	468 (590), 545 (162), 571 (137), 1237 (23)		
2	440 (467), 523 (170), 542 (121), 565 (64), 608 (21), 1262 (33)	1587, 1434	153
3	456 (6434), 710 (1277)	1575, 1424	151
4	465 (12037), 640 (2664)	1525, 1427	98
5	445 (487), 524 (193), 544 (138), 567 (80), 606 (36), 1259 (43)	1576, 1407	169
6	458 (6604), 710 (1330)	1558, 1391	167
7	467 (11598), 637 (2593)	1508, 1388	120
8	441 (521), 526 (176), 543 (144), 563 (78), 606 (40), 1253 (41)	1630, 1336	294
9	450 (5944), 684 (1287)	1610, 1344	266
10	466 (9000), 643 (2084)	1556, 1353	203

[a] The UV/vis and IR spectra were taken using the perchlorate salts. [b] Spectra were recorded in CH_3CN solution at 295 K. Concentration of solutions were ~1.0×10^{-3} for $Co^{II}Co^{II}$ forms and ~1.0×10^{-5} for $Co^{II}Co^{III}$ and $Co^{III}Co^{III}$ complexes. [c] $\Delta = \nu_{as} - \nu_s$. [d] Reference 32.

The mixed-valent complexes are very stable to disproportionation, as quantified by the comproportionation constants K_c defined for the equilibrium shown in eq 6.

$$[(L^{Me})Co^{II}_2(\mu\text{-}O_2CR)]^+ + [(L^{Me})Co^{III}_2(\mu\text{-}O_2CR)]^{3+} = 2[(L^{Me})Co^{II}Co^{III}(\mu\text{-}O_2CR)]^{2+}\ K_c \quad (6)$$

These constants are calculated by using the expression in eq 7

$$\Delta E = |E^1_{1/2} - E^2_{1/2}| = (RT/nF)\ln(K_c) \quad (7)$$

where ΔE is the separation of potentials for successive one-electron processes in volts.[49]

The comproportionation constants are in the range (1.81−2.67) × 10^6, showing no significant disproportionation of the mixed-valent species **3**, **6**, and **9**. Because of negligible

(49) See, for example: Flanagan, J. B.; Margel, S.; Bard, A. J.; Anson, F. C. *J. Am. Chem. Soc.* **1978**, *100*, 4248−4253.

metal−metal interactions (see below), the large ΔE values must be attributed to other factors such as electrostatic effects.[50]

Numerous mono- and binuclear cobalt(III) amine thiolate complexes have been prepared prior to this work,[33−40] and their electrochemical properties have been reported. There are no previous examples in which all three members of binuclear cobalt amine thiolate complexes have been isolated and structurally characterized (with the same ligand). For example, the binuclear complexes $[(L')_3Co^{III}_2]^{3+}$ **11** and $[(L'')Co^{III}_2]^{3+}$ **12**, where HL′ and H_3L'' represent the multidentate amine thiophenolate ligands 2,6-bis(aminomethyl)-4-*tert*-butylthiophenol and *N*,*N*′,*N*″-tris[2-thio-3-aminomethyl-5-*tert*-butylbenzyl]-1,1,1-tris(aminomethyl)ethane, respectively, have been isolated, but only in their $Co^{III}Co^{III}$ forms.[40] The redox potentials of **11** and **12** are shifted by ca. 1 V to more negative values, relative to those of the complexes described in this study. The shifts in the redox potentials are consistent with the change of the donor set from CoN_3S_2O in **2**−**10** to CoN_3S_3 in **11** and **12**. The large cathodic shifts cannot be explained by the change of donor atoms in the bridging region of the two metal ions alone. For example, the replacement of one bridging thiophenolate function in **11** to a bridging carboxylate ligand in **2** can be estimated to shift the $Co^{III/II}$ potentials by not more than ca. +0.50 V.[51] Clearly, the conversion of the terminal amine nitrogen donor atoms from secondary in **11** and **12** to tertiary in **2**−**10** must also be taken into account.

Spectroscopic Properties of 2−10. UV/vis Spectroscopy. The electronic absorption spectra of the complexes have been recorded in the range 300−1600 nm in acetonitrile solution at ambient temperature. The spectra of complexes **2**−**4** are representative for all other complexes; they are displayed in Figure S2 (Supporting Information). The UV/vis spectral data are reported in Table 3.

The spectra of the pale red Co^{II}_2 complexes are very similar and display typical weak d−d transitions of octahedral high-spin cobalt(II) (d^7) in the 300−1600 nm range.[52,53] Three spin-allowed d−d transitions are expected ($^4T_{1g}(F) \rightarrow {}^4T_{1g}(P)$, $^4T_{1g}(F) \rightarrow {}^4A_{2g}$, and $^4T_{1g}(F) \rightarrow {}^4T_{2g}$); however, the $^4T_{1g}(P)$ and $^4A_{2g}$ levels are usually of the same energy and the transitions to these two levels are close together.[52] The assignment of the weak band at ∼1260 nm to the $^4T_{1g}(F) \rightarrow {}^4T_{2g}$ transition is unequivocal. The more intense band at ∼450 nm most probably arises from a thiolate-to-cobalt(II) charge transfer (LMCT) transition. All cobalt(II) complexes display an absorption band at ∼520 nm with three shoulders at ∼540, 565, and 600 nm. These bands are attributable to components of the parent octahedral ligand field transitions, $^4T_{1g}(F) \rightarrow {}^4T_{1g}(P)$ and $^4T_{1g}(F) \rightarrow {}^4A_{2g}$, split by lower symmetry.

The UV/vis spectra of the mixed-valent $Co^{II}Co^{III}$ complexes and the fully oxidized $Co^{III}Co^{III}$ species are dominated by strong thiophenolate-to-cobalt(III) charge transfer transitions at ∼460 and 710 nm and at ∼465 and 640 nm, respectively. Intense LMCT transitions are characteristic of thiolate-bridged cobalt complexes, particularly for the more oxidized states.[32−40] The LMCT transitions of the fully oxidized complexes are approximately twice the intensity of the charge transfer transitions of the $Co^{II}Co^{III}$ forms, consistent with the presence of two $Co^{III}N_3S_2O$ chromophores in the former and only one such chromophore in the latter species.

From the X-ray data described below one could expect a superposition of the spectra of the constituent $N_3Co^{II}S_2O$ and $N_3Co^{III}S_2O$ ions for the mixed-valent species **3**, **6**, and **9**. Such a situation with distinct localized Co^{II} and Co^{III} sites would correspond to class I in Robin and Day's classification of mixed-valence species.[54,55] In the other extreme (class IIIa mixed-valence species featuring strong metal−metal interactions) the properties of the component species are replaced by those of a new delocalized species. Between these two extremes lies a wide range of intermediate cases with many gradations of metal−metal interactions (class II). However, due to the intense ligand-to-metal charge transfer transitions in the UV/vis spectra of the mixed-valent species (which would obscure any of the rather weak d−d transitions of a distinct localized Co^{II} ion), UV/vis spectroscopy is not suited to position the complexes in this scale. In addition, there are no additional bands (in the 300−1600 nm region) which could be attributable to intervalence transfer (IT) bands. It should, however, be noted that these bands can be very weak and situated in different areas of the spectrum, from the visible to the mid-IR.[56]

^{1}H NMR Spectroscopy. The complexes **2**, **4**, **5**, and **7** were further characterized by ^{1}H NMR spectroscopy. The ^{1}H NMR chemical shifts are reported in the Experimental Section. The ^{1}H NMR spectra obtained for the dicobalt(II) complexes **2** and **5** in CD_3CN solutions at 293 K are broad with chemical shifts ranging from +200 to −70 ppm, a range that is consistent with the presence of paramagnetic compounds.[57] The spectrum of **2** shows only 11 resonances, indicative of local C_{2v} symmetry of the monocation in solution. The resonances at 200.5, 147.4, 77.8, 76.9, −53.0, and −66.0 ppm can be assigned to the six nonequivalent methylene protons, whereas signals at 132.5 and 36.1 ppm are due to protons of the two nonequivalent NCH_3 groups. The aromatic protons resonate at 22.3 ppm, and the *t*-Bu groups give rise to a signal at 8.4 ppm. The corresponding resonances for **5** were observed at nearly the same values. The highly deshielded signal at 178.5 ppm in the spectrum of **2** is assigned to the CH_3 protons of the bridging acetate group, on the basis of both its relative integration and the absence of this signal in the spectrum of complex **5**. The

(50) Sutton, J. E.; Taube, H. *Inorg. Chem.* **1981**, *20*, 3125−3134.
(51) Krüger, H.-J.; Holm, R. H. *J. Am. Chem. Soc.* **1990**, *112*, 2955−2963.
(52) Cotton, F. A.; Wilkinson, G.; Murillo, C. A.; Bochmann, M. *Advanced Inorganic Chemistry*, 6th ed.; John Wiley & Sons: New York, 1999.
(53) Figgis, B. N. *Introduction to Ligand Fields*; Interscience: New York, 1986.
(54) Creutz, C. *Prog. Inorg. Chem.* **1983**, *30*, 1−73.
(55) Robin, M. B.; Day, P. *Adv. Inorg. Chem. Radiochem.* **1967**, *10*, 247−422.
(56) Kaim, W.; Bruns, W.; Kohlmann, S.; Krejcik, M. *Inorg. Chim. Acta* **1995**, *229*, 143−151.
(57) Bertini, I.; Luchinat, C.; Parigi, G. Solution NMR of Paramagnetic Molecules, Current Methods. In *Inorganic Chemistry*; Elsevier: Amsterdam, 2001; Vol. 2.

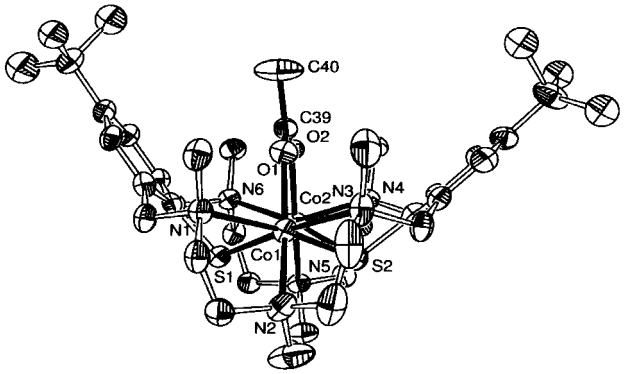

Figure 1. Perspective view of the cation $[(L^{Me})Co^{II}_2(\mu\text{-}O_2CMe)]^+$ in crystals of **2**·BPh_4. Atoms are drawn at the 50% probability level. Hydrogen atoms are omitted for clarity.

signals for the protons of the cinnamate ion in **5** are also deshielded. The deshielding of the protons increases (18.72, 18.76, 39.81, 106.9 ($CO_2CH{=}C\mathit{H}$), 185.7($CO_2C\mathit{H}{=}CH$)) with decreasing distance from the paramagnetic cobalt(II) ions.

In contrast, the signals in the ^{1}H NMR spectra of **4** and **7** under the same conditions are observed in the range 0−11 ppm, which is normal for Co^{III} compounds with low-spin d^6 configuration. For **4**, the aromatic and the *tert*-butyl protons appear as sharp singlets at 7.31 and at 1.22 ppm, again indicative of local C_{2v} symmetry in solution. Unfortunately, the signals in the 2.0−4.5 ppm region could not be assigned. It should be noted that the signal for the methyl protons of the coordinated acetate group is at 1.00 ppm, whereas this signal is observed at 1.83 ppm for sodium acetate.[32] The shift changes to a higher field can be explained by the fact that the coligand is situated in the hydrophobic binding pocket (i.e., the shielding region of the two aryl rings of $(L^{Me})^{2-}$). The signals for the two olefinic CH protons of the cinnamate ion in **7** at 6.63 and 5.84 are also shifted downfield from their values in sodium cinnamate (which are observed at 7.65, 6.53 ppm in CD_3CN).

The ^{1}H NMR spectrum of the mixed-valent species **3** was less informative. The signals at 3.8 and 23.4 ppm were sharp singlets. Further very broad signals were observed at 7.15, 12.7, and−29.2 ppm, while signals at ∼77, 65, and 42 ppm were only just above the baseline level.[58]

Descriptions of the Crystal Structures. The crystal structures of complexes **2**·BPh_4·MeCN, **3**·$(I_3)_2$, **5**·BPh_4·2MeCN, **6**·$(ClO_4)_2$·EtOH, **7**·$(ClO_4)_3$·MeCN·$(H_2O)_3$, and **9**·$(ClO_4)_2$·$(MeOH)_2$·H_2O were determined by single-crystal X-ray crystallography at 210 K. Suitable crystals of **4**·$(ClO_4)_3$ and of **10**·$(ClO_4)_3$ were not obtained. The structures of the complexes are similar to one another. The structures of **2** and **7** are shown in Figures 1 and 2. The structures of the other complexes are shown in Figures S3−S6 of the Supporting Information. Table 4 lists the individual metal−ligand bond lengths and gives information about selected C−O and C−C distances of the coligands. All other bond distances and angles are available in the Supporting Information. The atomic numbering scheme for the central $N_3Co(\mu\text{-}S)_2(\mu\text{-}O_2CR)CoN_3$ core in **2**·BPh_4 is depicted in Table 4. This was used for all compounds.

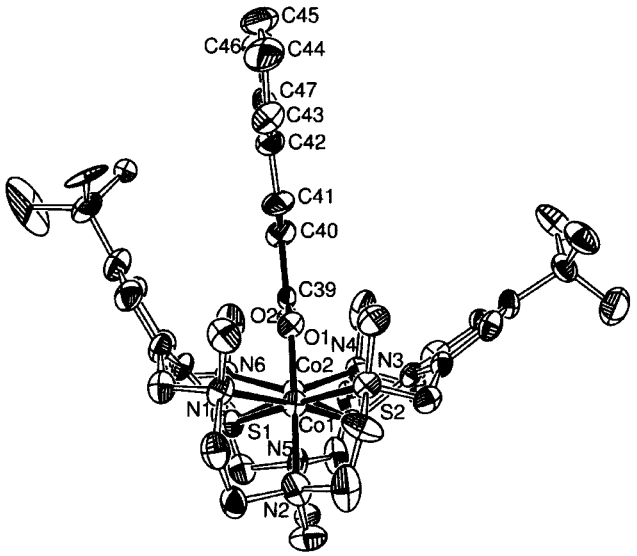

Figure 2. Perspective view of the cation $[(L^{Me})Co^{III}_2(\mu\text{-}O_2CCH{=}CHPh)]^{3+}$ in crystals of **7**·$(ClO_4)_3$. Atoms are drawn at the 50% probability level. Hydrogen atoms are omitted for clarity.

The crystal structure of **2**·BPh_4·MeCN is composed of discrete $[(L^{Me})Co^{II}(\mu\text{-}O_2CMe)]^+$ cations, tetraphenylborate anions, and acetonitrile molecules of solvent of crystallization. The structure of the cation is that of type B. The position X is occupied by an acetate group. It bridges the two Co^{II} centers in a symmetrical μ-1,3 fashion, at a distance of 3.448(1) Å. The idealized symmetry is C_s with a mirror plane passing through the two S atoms and the carboxyl carbon atom of the acetate group. Both cobalt atoms are six-coordinate with considerably distorted pseudooctahedral geometry. The corresponding bond lengths at Co(1) and Co(2) differ only slightly, but the individual Co−N and Co−S bond lengths vary widely. The Co(1)−N(2) and the Co(2)−N(5) bonds at 2.188(3) and 2.195(3) Å, respectively, are the shortest Co−N bonds; both are in a trans position relative to the coligand. The Co(1)−N(1) and Co(2)−N(6) bonds at 2.345(3) and 2.335(3) Å, respectively, are the longest Co−N bonds; both are in a trans position relative to the two short Co−S bonds at 2.475(1) and 2.472(1) Å. The remaining two Co−N bonds at 2.277(3) and 2.285(3) Å are in a trans position to the long Co−S bonds. Remarkably, the same pattern is found in the corresponding acetato-bridged complexes of Mn^{II},[59] Fe^{II},[59] Ni^{II}, and Zn^{II},[32] which are all isostructural with **2**. This is also observed for **3**, **5**, **6**, **7**, **8**,[32] and **9**. The observed differences in the individual Co−N and Co−S distances can therefore be attributed to steric constraints of the macrocyclic ligand, rather than to a specific metal d^n electronic configuration. Finally, the C−O distances at 1.258(4) and 1.264(4) Å are identical within

(58) Preliminary EPR measurements confirm that the Co^{II}_2 and $Co^{II}Co^{III}$ complexes **2** and **3** are paramagnetic species. The $Co^{III}Co^{III}$ complex is EPR silent. The EPR spectrum of **3** (Figure S7, Supporting Information) reveals a strong signal centered at $g_{av} > \sim 4.0$ indicative of an $S = 3/2$ spin ground state. We anticipate a more detailed study of the electronic structures of compounds **2** and **3** by temperature-dependent magnetic susceptibility measurements.

(59) Kersting, B.; Steinfeld, G. Unpublished results.

Table 4. Selected Bond Lengths of Cobalt Complexes **2**, **3**, **5**, **6**, **7**, and **9**

	2	**3**	**5**	**6**[a]	**7**	**9**
Co(1)–O(1)	2.011(2)	1.998(3)	2.020(2)	1.995(5) [2.029(5)]	1.851(9)	2.040(5)
Co(1)–N(1)	2.345(3)	2.242(3)	2.352(3)	2.228(6) [2.210(7)]	2.179(11)	2.270(7)
Co(1)–N(2)	2.188(3)	2.175(4)	2.199(3)	2.135(6) [2.172(6)]	2.048(12)	2.148(7)
Co(1)–N(3)	2.277(3)	2.188(4)	2.282(3)	2.284(6) [2.243(7)]	2.119(11)	2.191(7)
Co(1)–S(1)	2.525(1)	2.547(2)	2.516(1)	2.510(2) [2.528(2)]	2.310(4)	2.534(2)
Co(1)–S(2)	2.475(1)	2.426(1)	2.475(1)	2.516(2) [2.520(2)]	2.255(4)	2.484(2)
Co(2)–O(2)	2.015(2)	1.904(3)	2.022(2)	1.908(5) [1.881(5)]	1.876(9)	1.892(5)
Co(2)–N(4)	2.285(3)	2.137(4)	2.319(3)	2.126(6) [2.184(6)]	2.069(11)	2.157(6)
Co(2)–N(5)	2.195(3)	2.078(4)	2.195(3)	2.035(6) [2.013(7)]	2.045(11)	2.020(7)
Co(2)–N(6)	2.335(3)	2.219(4)	2.322(3)	2.193(6) [2.183(6)]	2.191(10)	2.175(6)
Co(2)–S(1)	2.537(2)	2.357(1)	2.563(1)	2.329(2) [2.313(2)]	2.319(4)	2.328(2)
Co(2)–S(2)	2.472(1)	2.310(1)	2.452(1)	2.323(2) [2.306(2)]	2.261(4)	2.309(2)

[a] There are two crystallographically independent molecules A and B in the unit cell. Values in square brackets refer to the corresponding bond lengths of molecule B. [b] R = CHPh.

Scheme 3. Schematic Representation of the Binding Mode of the Cinnamate Ion in **5**−**7**

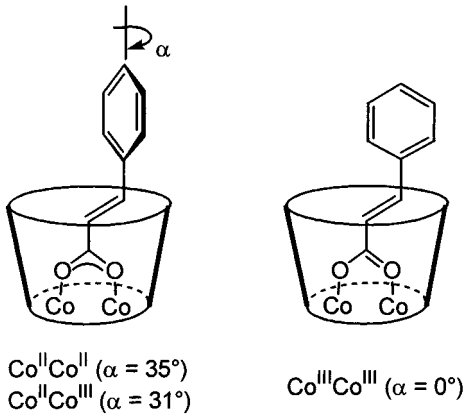

$Co^{II}Co^{II}$ (α = 35°)
$Co^{II}Co^{III}$ (α = 31°)
$Co^{III}Co^{III}$ (α = 0°)

experimental error; they are typical for bridging acetate groups.[15,60,61]

The crystal structure of **5**·BPh_4·2MeCN consists of discrete $[(L^{Me})Co^{II}_2(\mu\text{-}O_2CCH{=}CHPh)]^+$ cations, tetraphenylborate anions, and acetonitrile molecules of solvent of crystallization. Again, the structure of the cation is of the form B (Figure S4, Supporting Information). The cinnamate ion bridges the two six-coordinate Co^{II} ions in a symmetrical μ-1,3 fashion. The substituents at the carbon−carbon double bond are in a trans position. Note that the cinnamate ion is not planar. The phenyl ring is twisted by 35° relative to the alkene plane (Scheme 3). Table 4 shows that the respective metal−ligand bond lengths are essentially identical with those found for **2**. The average Co−N bond length of 2.278(3) Å is significantly longer than in $[Co^{II}(NH_3)_6]Cl_2$,[62] at 2.170(2) Å, and $[Co^{II}(tacn)_2]I_2$,[63] at 2.155(15) Å (tacn = 1,4,7-triazacyclononane), but comparable to literature values for cobalt(II) complexes with this macrocyclic amine thiophenolate ligand.[32] The cis and trans L−Co−L bond angles deviate by as much as 20° (for O(1)−Co−N(2), O(2)−Co(2)−N(5)) from their ideal values. As in **2**, the distortions can be traced back to the inflexible ligand geometry.

The crystal structure of **3**·$(I_3)_2$ consists of discrete $[(L^{Me})Co^{II}Co^{III}(\mu\text{-}O_2CMe)]^{2+}$ cations (Figure S3, Supporting Information) and I_3^- anions. When the different oxidation states of the cobalt ions in the dication **3** are neglected, the complex can be regarded as isostructural with its parent dicobalt(II) complex. Thus, oxidation of **2** does not affect its overall bowl-shaped structure and occurs without loss of the bridging coligand. The different metal−ligand bond lengths for the two cobalt centers reflect the mixed-valent nature of the complex and the metal-centered nature of the oxidation of **2**. The dication is assigned a $N_3Co^{II}(\mu\text{-}SR)_2(\mu\text{-}O_2CMe)Co^{III}N_3$ core structure with high-spin Co^{II} (Co(1)) and low-spin Co^{III} (Co(2)) ions, because the Co(1)−ligand distances are comparable with those of **2**, a complex which comprises of two high-spin Co^{II} ions. The average Co(2)−N and Co(2)−S bond lengths, at 2.145 and 2.334 Å, and the Co(2)−O(2) distance of 1.904(3) Å are all short, confirming this assignment. These distances are too short for an octahedral Co^{II} complex, but are in excellent accord with those of related low-spin $Co^{III}N_{6-x}S_x$[64,65] and $Co^{III}N_3S_2O$[66] complexes. The individual bond lengths and angles of the two thiophenolate head units in $(L^{Me})^{2-}$ show no unusual features and are almost identical with those in **2**. This rules out the possibility that the ligand is coordinated as a thiyl radical.[67]

(60) Turowski, P. N.; Armstrong, W. H.; Liu, S.; Brown, S. N.; Lippard, S. J. *Inorg. Chem.* **1994**, *33*, 636−645.
(61) Aquino, M. A. S. *Coord. Chem. Rev.* **1998**, *170*, 141−142.
(62) Newman, J. M.; Binns, M.; Hambley, T. W.; Freeman, H. C. *Inorg. Chem.* **1991**, *30*, 3499−3502.
(63) Küppers, H.-J.; Neves, A.; Pomp, C.; Ventur, D.; Wieghardt, K.; Nuber, B.; Weiss, J. *Inorg. Chem.* **1986**, *25*, 2400−2408.
(64) Tyler, L. A.; Noveron, J. C.; Olmstead, M. M.; Mascharak, P. K. *Inorg. Chem.* **2000**, *39*, 357−362.
(65) Higgs, T. C.; Ji, D.; Czernuszewicz, R. S.; Matzanke, B. F.; Schünemann, V.; Trautwein, A. X.; Helliwell, M.; Ramirez, W.; Carrano, C. J. *Inorg. Chem.* **1998**, *37*, 2383−2392.
(66) Klingele, M. H.; Steinfeld, G.; Kersting, B. *Z. Naturforsch., B* **2001**, *56b*, 901−907.

The crystal structure of **6**·$(ClO_4)_2$ reveals the presence of discrete $[(L^{Me})Co^{II}Co^{III}(\mu\text{-}O_2CCH{=}CHPh)]^{2+}$ dications (Figure S5, Supporting Information). There are two crystallographically independent molecules in the asymmetric unit. Since the two structures are essentially identical, the description will focus on molecule A. Unlike **5**, the cinnamate ion bridges the two Co atoms in an asymmetric manner, because of short Co(III)−O and long Co(II)−O distances. The C−O bond lengths are, however, uniform, indicative of a sp^2-hybridized carboxylate function, as is observed in the parent $Co^{II}Co^{II}$ form **5**. Likewise, the phenyl ring of the cinnamate ion is twisted out of the alkene plane, albeit to a lesser degree (31°). The cation has the same average Co−N and Co−S distances as observed in the mixed-valent $Co^{II}Co^{III}$ species **3**. Thus Co(1) can be assigned an oxidation state +II (d^7, high spin) and Co(2) an oxidation state +III (d^6, low spin).

The X-ray structure analysis of **7**·$(ClO_4)_3$ shows the presence of discrete $[(L^{Me})Co^{III}_2(\mu\text{-}O_2CCH{=}CHPh)]^{3+}$ trications of the structure type B. This result confirms unambiguously that the overall structure of the parent complexes is retained in all three oxidation states (Figure 2). However, there are several differences that are worth considering. First, the short average Co−N and Co−S distances (for Co(1) 2.115(3) and 2.283(4) Å, for Co(2) 2.102(3) and 2.290(3) Å) together with the short Co−O bond lengths at 1.851(9) and 1.876(9) Å are now only compatible with a low-spin d^6 configuration for both Co atoms. Second, the cinnamate ligand shows a short C−O distance at 1.24(2) Å (C(39)−O(1)) and a long C(39)−O(2) bond at 1.35(2) Å, indicating partial double-bond character for the C(39)−O(1) bond. Third, the cinnamate ion is almost planar (the maximum deviations from the best least-squares plane are at 0.02 Å). This is a striking contrast to the twisted conformations found in the two reduced forms. Clearly, the binding mode (the electronic structure) of the carboxylate ligands is a function of the oxidation states of the two metal ions. The observed trends are fully consistent with the observed shifts in vibrational frequencies across the series (see below).

It should be noted that the presence of asymmetric RCO_2^- bridges is unusual for carboxylato-bridged dicobalt(III) complexes. For example, the carboxylate substituents in $[\{(tacn)Co\}_2(\mu\text{-}OH)_2(\mu\text{-}O_2CMe)]^{3+}$ and $[\{(NH_3)_3Co\}_2(\mu\text{-}OH)_2(\mu\text{-}O_2CR)]^{3+}$ assume uniform C−O bond lengths which are only compatible with sp^2-hybridized carboxylate functions.[68,69] In the present Co^{III}_2 complexes, the bonding situation of the carboxylates allows for assuming a coordinated carbonyl group (C(39)=O(1)) and an sp^3-hybridized oxygen atom (C(39)−O(2)) as in carboxylic acids (RCOOH). The differences may be attributed to ligand constraints or to the more hydrophobic microenvironment about the positively charged Co^{III} centers and the negatively charged carboxylate ligands. It is well-known that Coulombic forces increase with decreasing dielectric constant of the medium.[70] Clearly, more data are needed to further investigate these phenomena.

Crystals of **9**·$(ClO_4)_2$ consist of $[(L^{Me})Co^{II}Co^{III}(\mu\text{-}O_2COMe)]^{2+}$ cations (Figure S6, Supporting Information) and well-separated ClO_4^- anions. The metal−ligand bond lengths compare well with those observed for the $Co^{II}Co^{III}$ complexes **3** and **6**. Further details of the structure may be found in the Supporting Information.

Infrared Spectroscopy. The infrared spectra of **2**−**10** display the bands expected for the macrocyclic amine ligand $(L^{Me})^{2-}$, counterions (ClO_4^-), and carboxylate and alkyl carbonate coligands. The ClO_4^- ions give rise to a broad band at 1100 cm^{-1}, which is normal for this counterion. Each spectrum displays two further strong absorptions in the 1650−1300 cm^{-1} region, which are associated with the asymmetric (ν_{as}(C−O)) and symmetric stretching modes (ν_s(C−O)) of the carboxylate and alkyl carbonate coligands, respectively.[71] The observed values for ν_{as} and ν_s for the dicobalt(II) complexes **2** and **5** are typical for symmetrical carboxylate bridges. The separations ($\Delta = \nu_{as} - \nu_s$) between the two C−O stretching frequencies at 153 and 169 cm^{-1} are also normal.[71,72] As can be seen in Table 3, the corresponding frequencies in the mixed-valent species **3** and **6** are all shifted slightly to lower frequencies (by maximal 18 cm^{-1}) with the Δ values remaining essentially unchanged. Upon conversion to the $Co^{III}Co^{III}$ forms, the C−O stretching frequencies are much more affected; in particular, the ν_{as} values are shifted by 50 cm^{-1} to lower wavenumbers when compared with the corresponding values of the reduced members of the respective series. Note that the same trend is observed in the methyl carbonato complexes **8**, **9**, and **10**. The decreases in C−O stretching frequencies upon conversion from the Co^{II}_2 to the Co^{III}_2 forms are indicative of weaker C−O bonds in the oxidized $Co^{III}Co^{III}$ complexes. This is consistent with the results from the X-ray crystal structure determinations described above. The conclusion that emerges is that nucleophilic substitutions at the carboxyl carbon atoms of the substrates, in particular for those of the alkyl carbonates, should become more feasible in the fully oxidized forms.[73] Kinetic studies are underway to explore the chemical reactivity of the complexes as a function of the metal oxidation states.

Conclusion

The carboxylato and methyl carbonato bridged dicobalt complexes **2**−**10** are redox-active species that undergo two stepwise one-electron-oxidation processes. All three members of each series are cleanly obtained by chemical oxidation of the parent $Co^{II}Co^{II}$ forms by using mild oxidants. The monooxidized complexes are mixed-valent $Co^{II}Co^{III}$ compounds with localized high-spin Co^{II} (d^7) and low-spin Co^{III} (d^6) ions. The fully oxidized forms represent diamagnetic

(67) Kimura, S.; Bothe, E.; Bill, E.; Weyhermüller, T.; Wieghardt, K. *J. Inorg. Biochem.* **2001**, *86*, 294.
(68) Wieghardt, K.; Schmidt, W.; Nuber, B.; Weiss, J. *Chem. Ber.* **1979**, *112*, 2220−2230.
(69) Maas, G. *Z. Anorg. Allg. Chem.* **1977**, *432*, 203−210.
(70) Zubay, G. L. *Biochemistry*, 4th ed.; McGraw-Hill: New York, 1998.
(71) Nakamoto, K. *Infrared and Raman Spectra of Inorganic and Coordination Compounds*, 5th ed.; Wiley: New York, 1997.
(72) Deacon, G. B.; Phillips, R. J. *Coord. Chem. Rev.* **1980**, *33*, 227−250.
(73) Wahnon, D.; Lebuis, A.-M.; Chin, J. *Angew. Chem., Int. Ed. Engl.* **1995**, *34*, 2412−2416.

Co^{III}_2 species with low-spin d^6 configuration for both Co^{III} ions. The metal-centered redox reactions do not affect the overall bowl-shaped structure of the parent complexes, the coligands remain in a bridging position, and the solid-state structures are retained in the solution state. Infrared spectral changes that occur upon oxidation of the complexes suggest that the substrates are more susceptible to nucleophilic attack by the solvent or other reagents.

Acknowledgment. This work was supported by the Deutsche Forschungsgemeinschaft (Project No. KE 585/3-1). We are particulary grateful to Prof. Dr. H. Vahrenkamp for his generous and continuous support. The authors thank Gabriel Siedle for recording NMR spectra and Emma Craven for reading the manuscript.

Supporting Information Available: Six X-ray crystallographic files for **2**, **3**, **5**, **6**, **7**, and **9** in CIF format; Figure S1 of the cyclic voltammogram of compound 2; Figure S2 of the electronic absorption spectra of complexes **2**−**4**; Figures S3−S6 of the molecular structures of complexes **3**, **5**, **6**, and **9**; Figure S7 of the EPR spectra of complexes **2** and **3**. This material is available free of charge via the Internet at http://pubs.acs.org.

IC011004N